GMR Genetics and Molecular Research
Online Journal
ISSN:1676-5680

Cytochalasin B inhibits the proliferation of human glioma U251 cells through cell cycle arrest and apoptosis

Z.G. Tong[1], N. Liu[2], H.S. Song[2], J.Q. Li[2], J. Jiang[2], J.Y. Zhu[2] and J.P. Qi[2]

[1]Department of General Surgery,
Fourth Affiliated Hospital of Harbin Medical University, Nangang District, Harbin, China
[2]Department of Pathology,
First Affiliated Hospital of Harbin Medical University, Nangang District, Harbin, China

Corresponding author: J.P. Qi
E-mail: 252302504@qq.com

Genet. Mol. Res. 13 (4): 10811-10822 (2014)
Received January 3, 2014
Accepted June 26, 2014
Published December 19, 2014
DOI http://dx.doi.org/10.4238/2014.December.19.2

ABSTRACT. Cytochalasin B (CB) is known to inhibit a number of cancer types, but its effects on gliomas are unknown. We examined the *in vitro* effects of CB on the proliferation of human glioma U251 cells, as well as determined its mechanism of action. Cell proliferation was determined using CCK-8. The effect of CB on U251 cell morphology was observed under a transmission electron microscope. Cell cycle distribution was assessed using propidium iodine and Giemsa staining, and cell apoptosis was determined by annexin V-fluorescein isothiocyanate/propidium iodide. Cell cycle-related proteins were determined by Western blot. CB effectively inhibited U251 cell proliferation in a dose- and time-dependent manner. The 24, 48, 72, and 96 h IC_{50} values were 6.41 x 10^{-2}, 9.76 x 10^{-4}, 2.57 x 10^{-5}, and 2.08 x 10^{-5} M, respectively. CB increased the proportion of cells in the G2/M phase in a dose-dependent manner, thus increasing the mitotic index and decreasing cdc2 and cyclin B1 protein levels. CB

induced morphological changes in the cytoskeleton. Additionally, 10^{-5} M CB induced apoptosis in 23.4 ± 0.5% of U251 cells ($P < 0.05$ *vs* control group). Caspase-3, -8, and -9 activities were increased after CB treatment. CB inhibited U251 glioma cell proliferation by damaging the microfilament structure. CB also induced glioma cell apoptosis, suggesting that it may be an effective therapeutic agent against gliomas.

Key words: Apoptosis; Cytochalasin B; Glioma; Mitosis

INTRODUCTION

Gliomas are rapidly progressing malignant brain tumors arising from glial cells, making up approximately 80% of all brain tumors (Mamelak and Jacoby, 2007; Goodenberger and Jenkins, 2012). Gliomas are aggressive tumors that can induce a variety of neurological symptoms depending upon the region of the brain affected (Chang et al., 2005). The prognosis can vary and is affected by age at presentation, tumor grade, and Karnofsky performance status, with survival ranging from a few months to a few years (Laws et al., 2003; Lamborn et al., 2004). Glioma treatment is typically multidisciplinary and involves maximal surgical resection, chemotherapy, and radiation therapy.

Cytochalasins are alkaloid mycotoxins widely present in fungi and extracted from the endophytic fungus *Rhinocladiella* sp found on the traditional Chinese medicinal plant *Tripterygium* (Haidle and Myers, 2004). Many types of cytochalasins have been identified, including cytochalasins A, B, C, D, H, and O (Haidle and Myers, 2004). They possess some important biological activities, such as the ability to inhibit mammalian cell division as well as protease, antibiosis, and antitumor activities (Espada et al., 1997). Cytochalasin B (CB) can pass through the cell membrane and bind to F-actin, which inhibits the superposition of G-actins and promotes cytoskeleton depolymerization (Zeng et al., 1997). The cytoskeleton affects cell morphology, cytoplasm flow, chromosome polymerization, and the location and directional movement of nuclei. During mitosis, the cytoskeleton also plays an important role in maintaining the polar distribution of the spindle, in the formation of the cleavage furrow, and in chromosome separation (Pollard and Cooper, 2009). Thus, the cytoskeleton depends on the dynamic balance of G-actin molecules; their polymerization/depolymerization is strictly regulated in normal cells. However, this balance is often disrupted in cancer cells, damaging the cytoskeletal structure and function. This imbalance may lead to higher sensitivity of cancer cells to CB, thereby inhibiting cancer cell proliferation (Ben-Ze'ev, 1985; Buendia et al., 1990; Stournaras et al., 1996; Li et al., 2011; Wang et al., 2011).

Although a number of studies have reported that CB affects the cell cycle, there are few reports regarding its role in inducing glioma cell apoptosis. Accordingly, we examined the effect of CB on glioma U251 cells *in vitro* by observing its inhibitory effect on cell survival and proliferation. Changes in the microfilaments of the cytoskeleton and their structures were also assessed.

MATERIAL AND METHODS

Cell culture

Human glioma U251 cells were obtained from the Cell Bank of the Chinese Academy

of Sciences (Shanghai, China). Cells were cultured in DMEM medium (Hyclone, Thermo Fisher Scientific, Waltham, MA, USA) supplemented with 10% fetal calf serum (Hangzhou Sijiqing Bioengineering Material Co., Ltd., Hangzhou, China), 10 kU/mL penicillin G, and 10 mg/mL streptomycin at 37°C in a humidified incubator with 5% CO_2.

CCK-8 assay

U251 cells were plated on 96-well plates at a density of 5 x 10^3 cells/well in a volume of 100 μL/well. Medium without cells was added to the blank control wells. Once the cells had adhered to the plates, CB (Sigma, St. Louis, MO, USA) was added at concentrations of 10^{-8}, 10^{-7}, 10^{-6}, 10^{-5}, 10^{-4}, 10^{-3}, 10^{-2}, and 10^{-1} M. CB was first dissolved in 100% dimethylsulfoxide, and then diluted in phosphate-buffered saline; the concentration of dimethylsulfoxide in the medium was <0.1%. The negative control contained <0.1% dimethylsulfoxide without CB (0 μM). After 24, 48, 72, and 96 h, 10 μL CCK-8 reagent (CCK-8 assay kit for measuring cell proliferation and cytotoxicity; Beyotime Institute of Biotechnology, Haimen, China) was added to the cells and incubated for 2 h. Absorbance was measured at 450 nm as optical density (OD) values using a KHB ST-360 microplate reader (Kehua Laboratory System Co., Ltd., Shanghai, China) (Espindola et al., 2000; White et al., 2001; Kong et al., 2011). The percentages of cell viability were calculated in each group using the following formula:
Cell viability (%) = ($OD_{experimental}$ - OD_{blank} / $OD_{control}$ - OD_{blank}) x 100%.

IC_{50} was calculated in each group using the FORECAST function in Microsoft Excel 2007.

Morphological examination by transmission electron microscope

U251 cells were treated with 10^{-5} M CB for 72 h and subsequently collected and fixed in 2.5% glutaraldehyde at 4°C for 30 min. Cells were centrifuged (9000 *g*, 10 min), fixed in 3% glutaraldehyde at 4°C for 1 h, dehydrated in gradient acetone, and embedded in Epon812. Resultant blocs were then sectioned into ultra-thin sections using an ultra-thin slicer (50 nm). Sections were stained with uranyl acetate and lead citrate for 5 min, followed by thorough washing with distilled water. Cytoskeletal microfilament changes in U251 cells were observed using a model H-600A transmission electron microscope (Hitachi, Tokyo, Japan).

Cell cycle distribution

U251 cells were treated with 10^{-8}, 10^{-7}, 10^{-6}, 10^{-5}, or 10^{-4} M CB for 72 h, after which the cells were collected. Cells were fixed in 70% ethanol overnight at 4°C. Next, 125 U/mL RNase A (Sigma) and 50 μg/mL propidium iodide (PI) (BD Pharmingen™, Franklin Lakes, NJ, USA) were added, and cells were incubated in the dark at 4°C for 30 min. Cells were analyzed using a FACS Calibur flow cytometer (BD Biosciences), and cell cycle distribution was calculated using the ModFit LT 3.2 software (BD Biosciences).

Giemsa staining

U251 cells (1 x 10^6 cells/well) were seeded on 60-mm culture plates containing coverslips, and were cultured for 5 days. The cells were then treated with 10^{-8}, 10^{-7}, 10^{-6}, 10^{-5}, or 10^{-4} M CB for 72 h. Cells were collected, fixed with 4% paraformaldehyde for 30 min, and stained

with Giemsa (Alfa Aesar B21172, Ward Hill, MA, USA) at 37°C for 30 min. After washing the cells with phosphate-buffered saline 3 times, they were treated with xylene for 5 min, sealed in neutral resin, and observed under a microscope (LEICA DM400, Solms, Germany). Ten fields from each coverslip were randomly selected. Mitotic index (%) = cell number in mitotic phase / total cells x 100%.

Cell apoptosis by dual-staining with annexin-V and PI

U251 cells were treated with 10^{-8}, 10^{-7}, 10^{-6}, 10^{-5}, or 10^{-4} M CB for 72 h. Cells were then harvested by centrifugation and resuspended in 1X binding buffer (cell density: 1 x 10^6 cells/mL). A 100-µL sample of this suspension was incubated with 5 µL annexin V-fluorescein isothiocyanate (Annexin-FITC Apoptosis Detection Kit, Beyotime Institute of Biotechnology) in the dark, at room temperature for 15 min. The volume was brought to 400 µL using 1X binding buffer. Next, 3 µL PI was added 5 min before conducting the measurement. Apoptosis was determined by flow cytometric analysis using a FACS Calibur flow cytometer. Annexin V was set as the x-axis and PI was set as the y-axis. Mechanically damaged cells were located in the upper left quadrant, apoptotic or necrotic cells in the upper right quadrant, dual negative and normal cells in the lower left quadrant, and early apoptotic cells in the lower right quadrant of the flow cytometric dot plot.

Western blot analysis

U251 cells were treated with 10^{-8}, 10^{-7}, 10^{-6}, 10^{-5}, or 10^{-4} M CB for 72 h. Cells were then collected and lysed with RIPA lysis buffer (Beyotime Institute of Biotechnology), according to manufacturer instructions. Proteins were quantified using a BCA Protein Assay Kit (Beyotime Institute of Biotechnology). For Western blot analysis, equal amounts of protein (45 µg) were separated by 12% sodium dodecyl sulfate-polyacrylamide gel electrophoresis and then electrophoretically transferred to nitrocellulose membranes (Beyotime Institute of Biotechnology). Non-specific sites were blocked with 5% milk powder diluted in Tris-buffered saline containing 0.05% Tween 20. Proteins were detected using the following antibodies: rabbit polyclonal antibody against cdc2, cyclin B1, and β-actin (Santa Cruz Biotechnology, Santa Cruz, CA, USA). After overnight incubation with the primary antibody, each blot was washed 4 times with Tris-buffered saline containing 0.05% Tween 20. Blots were then incubated with horseradish peroxidase-conjugated goat anti-rabbit secondary antibodies (Santa Cruz Biotechnology). Proteins were detected using an enhanced chemiluminescence reagent (Haigene Biotechnology, Heilongjiang, China). Band intensity was quantified using the ImageJ software (National Institutes of Health, Bethesda, MD, USA). Protein expression was normalized to that of β-actin.

Caspase-3, -8, and -9 activity assays

Activities of caspase-3, -8, and -9 were assessed using caspase-3, -8, and -9 Colorimetric Assay Kits (Beyotime Institute of Biotechnology), based on spectrophotometric detection of the color reporter molecule detection *p*-nitroanaline (pNA) after cleavage from the labeled substrates Ac-DEVD-pNA (caspase-3), Ac-IETD-pNA (caspase-8), and Ac-LEHD-pNA (caspase-9). Briefly, U251 cells were treated with 10^{-8}, 10^{-7}, 10^{-6}, 10^{-5}, or 10^{-4} M CB for

72 h. Cells (2 x 10^6) were then collected and were added to 100 μL lysis buffer on ice for 15 min. The lysate was then collected by centrifugation (16,000-20,000 *g*, 4°C, 10-15 min) and stored at -70°C until use. Protein concentration was determined using the Bradford method. Supernatant samples containing 10-30 μg total protein were used for caspase activity. Samples were added to 96-well microtiter plates with substrates at 37°C for 1-2 h. The optical density of each well was measured at 405 nm using a Model 550 microplate reader (Bio-Rad, Hercules, CA, USA). The results are reported as units, with 1 unit defined as the amount of enzyme cleaving 1.0 nmol colorimetric substrate per hour at 37°C under saturated substrate concentrations. Relative caspase activity (%) = caspase activity$_{experimental}$ / caspase activity$_{control}$ x 100%.

Statistical analysis

Each experiment in each group was repeated 3, 6, or 10 times. Data were analyzed using SPSS 17.0 (SPSS Inc., Chicago, IL, USA). Data are reported as means ± standard deviation. Data were analyzed using analysis of variance with the Student-Newman-Keuls test (heterogeneity of variance) or the Dunnett *t*-test (homogeneity of variance) for *post hoc* analysis. A P value <0.05 was considered to be statistically significant.

RESULTS

CB inhibited U251 cell proliferation

Increasing concentrations of CB increased the inhibition rates of U251 cell proliferation, compared to the control group (0 M). In addition, exposing the cells for a longer time enhanced the effects of CB on proliferation, but there was no difference between 72 and 96 h (P > 0.05; Figure 1). The 24, 48, 72, and 96 h IC_{50} values were 6.41 x 10^{-2}, 9.76 x 10^{-4}, 2.57 x 10^{-5}, and 2.08 x 10^{-5} M, respectively.

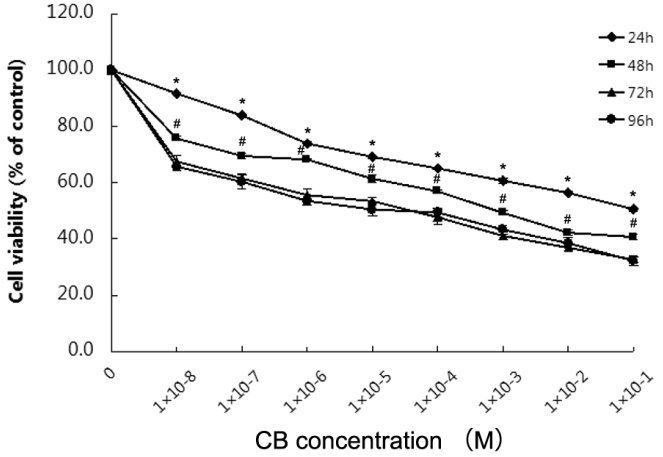

Figure 1. Viability curves of U251 cells treated with different concentrations of cytochalasin B (CB) (10^{-8}, 10^{-7}, 10^{-6}, 10^{-5}, 10^{-4}, 10^{-3}, 10^{-2}, and 10^{-1} M) for different durations (24, 48, 72, and 96 h). Cell proliferation was determined using a CCK-8 assay. Results are reported as means ± standard deviation obtained from 3 independent experiments.*P < 0.05 *vs* 24 h; #P < 0.05 *vs* 48 h.

CB induced G2/M phase U251 cell cycle arrest

In the control group, the proportion of U251 cells in G2/M phase was 10.4 ± 1.0%. In the presence of CB, the proportion of U251 cells in the G2/M phase increased with CB dose (10^{-8} M: 12.7 ± 1.0%; 10^{-7} M: 15.3 ± 1.5%; 10^{-6} M: 18.5 ± 0.7%; 10^{-5} M: 68.9 ± 1.4%; and 10^{-4} M: 64.2 ± 0.7%; all $P < 0.05$ *vs* the control group) (Figure 2).

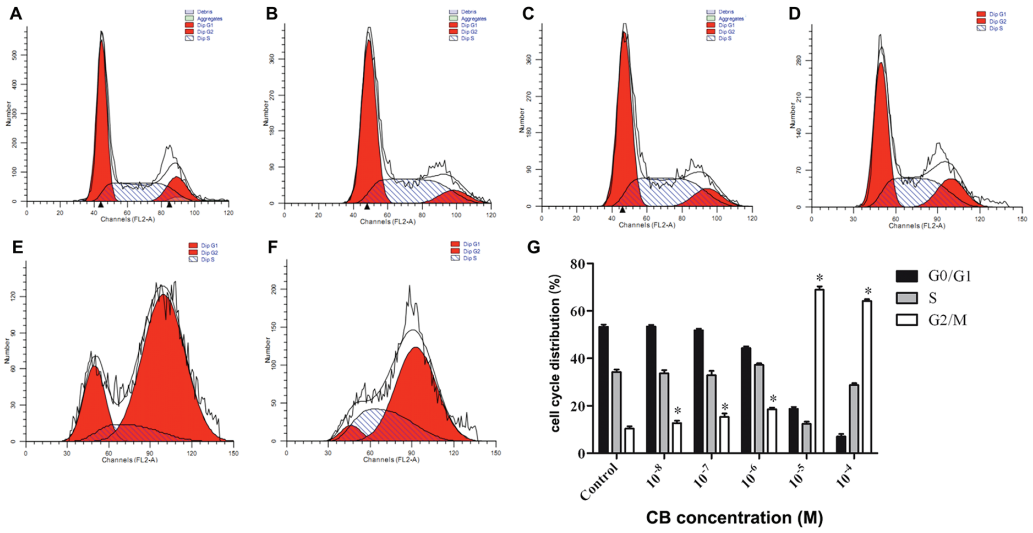

Figure 2. Effect of cytochalasin B (CB) on cell cycle distribution. Cell cycle was analyzed using propidium iodine staining and flow cytometry. Cells were treated with different concentrations of CB for 72 h. **A.** Control group. **B.** 10^{-8} M. **C.** 10^{-7} M. **D.** 10^{-6} M. **E.** 10^{-5} M. **F.** 10^{-4} M. **G.** Proportion of cells in G1/G0, S, and G2/M phases. Results are reported as means ± SD obtained from 6 independent experiments. *$P < 0.05$ *vs* the control group.

Giemsa staining revealed that the mitotic index was significantly increased using 10^{-5} M CB in U251 cells [13.8 ± 1.6% *vs* control (3.4 ± 2.0%), $P < 0.001$] (Figure 3).

Finally, Western blots showed that CB decreased cdc2 protein expression in a dose-dependent manner compared with control cells (control: 1.0; 10^{-8} M: 0.86 ± 0.07; 10^{-7} M: 0.61 ± 0.01; 10^{-6} M: 0.55 ± 0.04; 10^{-5} M: 0.24 ± 0.02; and 10^{-4} M: 0.20 ± 0.01), as well as cyclin B1 protein expression (control: 1.0; 10^{-8} M: 0.81 ± 0.01; 10^{-7} M: 0.57 ± 0.05; 10^{-6} M: 0.42 ± 0.03; 10^{-5} M: 0.26 ± 0.01; and 10^{-4} M: 0.13 ± 0.01) (Figure 4).

CB induced U251 cell apoptosis

After treatment for 72 h with 10^{-5} M CB, structural changes in the cytoskeletal microfilaments were observed under an electron microscope (Figure 5). In U251 cells without CB (the control group), cytoskeletal microfilaments showed a filamentous structure (Figure 5A) and were evenly distributed in the cytoplasm. After CB treatment, these microfilaments appeared as short rod-like structures (Figure 5B) or villi (Figure 5C). Apoptotic bodies were observed in approximately 10% of the cells (Figure 5D).

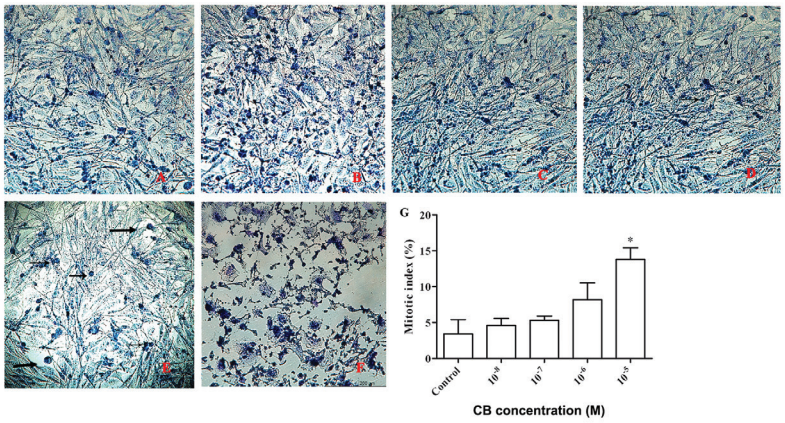

Figure 3. Effect of cytochalasin B (CB) on mitosis. Determination of the mitotic index using Giemsa staining. Cells were treated with different concentrations of CB for 72 h. **A.** control group. **B.** 10^{-8} M. **C.** 10^{-7} M. **D.** 10^{-6} M. **E.** 10^{-5} M. **F.** 10^{-4} M. Arrows show mitotic cells (20X). **G.** Mitotic indexes. Results are reported as means ± SD obtained from 10 independent experiments. *P < 0.001 *vs* the control group.

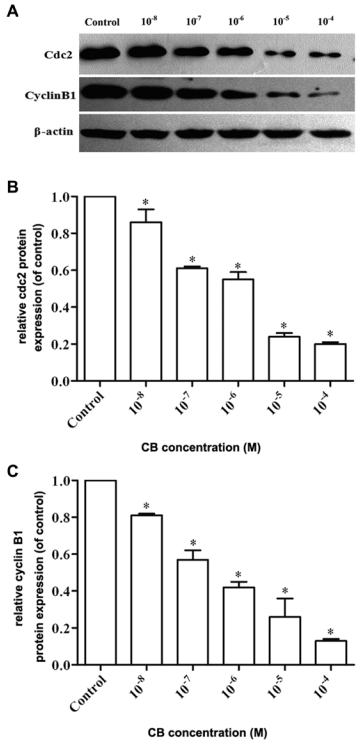

Figure 4. Western blot analysis of cdc2 and cyclin B1 protein expression. Cells were treated with different cytochalasin B (CB) concentrations (10^{-8}, 10^{-7}, 10^{-6}, 10^{-5}, and 10^{-4} M) for 72 h. **A.** Representative Western blot. β-actin was used as an internal control. **B.** Relative cdc2 protein expression (of control). **C.** Relative cyclin B1 protein expression (of control). The value of control group was 1.0. Results are reported as means ± SD obtained from three independent experiments. *P < 0.05 *vs* the control group.

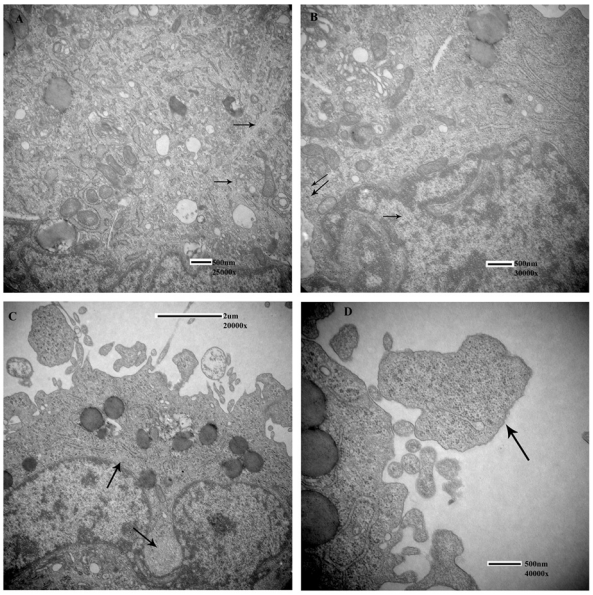

Figure 5. Electron microscopy of cytoskeletal microfilaments and apoptotic U251 cells after treatment with 10^{-5} M CB for 72 h. **A.** Microfilament structure (arrows) in normal U251 cells of the control group (25,000X). **B.** Microfilament in the shape of short rod-like structures (arrows) after CB treatment (30,000X). **C.** Microfilament in the shape of villi (arrows) after CB treatment (20,000X). **D.** An apoptotic body (arrow) (40,000X).

Using an annexin V-fluorescein isothiocyanate apoptosis detection kit, we showed that the proportions of cells in early apoptosis were increased following CB treatment, with the maximum effect reaching 10^{-5} M (control: 0.5 ± 0.2%; 10^{-8} M: 1.7 ± 0.2%; 10^{-7} M: 13.1 ± 0.4%; 10^{-6} M: 16.1 ± 0.3%; 10^{-5} M: 23.4 ± 0.5%; and 10^{-4} M: 21.2 ± 1.0%) (Figure 6).

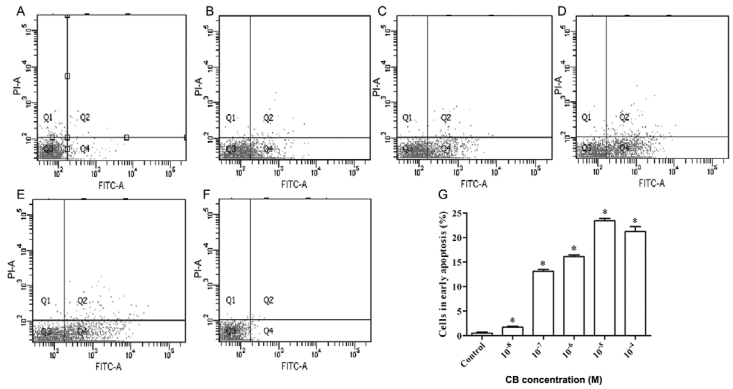

Figure 6. Effect of cytochalasin B (CB) on U251 cell apoptosis. Determination of the proportions of cells in early apoptosis using an annexin V-FITC/PI assay. Cells were treated with different concentrations of CB for 72 h. **A.** The control group. **B.** 10^{-8} M. **C.** 10^{-7} M. **D.** 10^{-6} M. **E.** 10^{-5} M. **F.** 10^{-4} M. **G.** Proportions of cells in early apoptosis. Results are shown as means ± SD obtained from 6 independent experiments. *P < 0.05 *vs* the control group. Q1: mechanically damaged cells; Q2: apoptotic or necrotic cells; Q3: dual-negative and normal cells; Q4: early apoptotic cells.

Finally, caspases-3, -8, and -9 activities were increased with CB concentration, with the maximum effect reaching 10^{-5} M (caspase-3: 228.3 ± 5.9%; caspase-8: 212.2 ± 5.7%; and caspase-9: 209.5 ± 4.6; all $P < 0.05$ *vs* control group) (Figure 7).

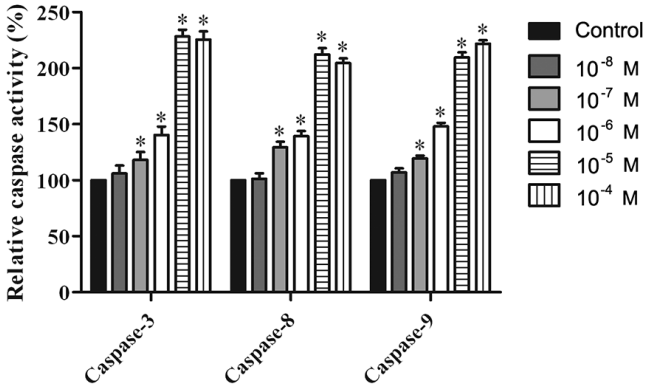

Figure 7. Effects of CB on caspase-3, -8, and -9 activities. U251 cells were treated with different concentrations of CB (10^{-8}, 10^{-7}, 10^{-6}, 10^{-5}, and 10^{-4} M) for 72 h. Results are reported as means ± SD obtained from 6 independent experiments. *$P < 0.05$ *vs* the control group.

DISCUSSION

Gliomas are malignant brain tumors with a poor prognosis. Few cytotoxic agents are currently available for treating these tumors. CB is known to inhibit a number of cancer types, but its effects on glioma cells are unknown. The aim of the present study was to assess the effects of CB on the glioma cell cycle and apoptosis.

The main result of this study was that CB inhibited human glioma U251 cells through cell cycle arrest and apoptosis in a dose- and time-dependent manner. Electron microscopy revealed that the cytoskeletal microfilaments in U251 cells were disrupted following CB treatment at 10^{-5} M for 72 h. CB induced apoptosis in approximately 10% of U251 cells, as indicated by the presence of apoptotic bodies. However, the inhibitory effects of CB on U251 cells were stronger than its cytotoxic effects. These results suggest that CB inhibited normal mitosis in U251 cells by disrupting the cytoskeleton. Indeed, recent studies revealed that the actin cytoskeleton participates in important cellular activities, such as cellular movement, substance transport, energy and message transmission, gene expression, cell division, differentiation and apoptosis, and the transition to cancer (Pollard and Cooper, 2009; Karp, 2010). Polymerization and depolymerization of actin molecules in the cell are closely related to cell proliferation and differentiation. Rapidly dividing tumor cells contain microfilaments with abnormal structures that can adapt to the active mitosis and increased proliferation (Pedersen et al., 2001). Similarly to a capping protein, CB selectively binds to the end of F-actin and inhibits the formation and microfilament cross-links while promoting the depolymerization of polymerized microfilaments (Cimini et al., 1998). Pedersen et al. (2001) found that CB depolymerized F-actin, thus inhibiting increases in tumor cell volume under different osmotic pressures. However, cytochalasin D showed no such effects. Their findings indicated that CB could also divide F-actin, as well as cause F-actin depolymerization. These effects are similar to those of other cancer drugs that act on the cytockeleton, such as taxanes (Kavallaris, 2010).

Our results showed that CB arrested human glioma U251 cells in the G2/M phase in a dose- and time-dependent manner, thus decreasing the mitotic index. These changes in the cell cycle were mediated, at least in part, by decreased expression of cdc2 and cyclin B1 proteins, 2 factors involved in the cell cycle. Indeed, cdc2 interacts with cyclins to lead cell cycle progression, controlling G1/S gene transcription (Skotheim et al., 2008). Furthermore, the cdc2/cyclin B1 complex is the main regulator of G2/M progression, controlling the activity of a number of proteins involved in cytoskeletal stability and spindle formation (Ohsugi et al., 2003). Cyclin B1 is essential for tumor cell survival, and its down-regulation lead to cell death (Yuan et al., 2004). Studies using paclitaxel to destabilize microtubules revealed that dysregulation of the cdc2/cyclin B1 complex was one of the events leading to paclitaxel-induced apoptosis (Huang et al., 2000). Thus, CB-induced cytoskeletal disruption impaired the formation of the mitotic spindle, blocking the cells in the G2/M phase. However, our results did not allow us to determine whether cdc2/cyclin B1 down-regulation was a consequence or a cause of this arrest, nor the exact relation of this decrease with the destabilization of microtubules. Similar results regarding cell cycle arrest were observed in liver and lung cancer cells (Liang et al., 2003; Chao and Liu, 2006).

Caspases play a central role in apoptosis. They can be classified as initiator caspases (such as caspase-8 and -9) and as effector caspases (such as caspase-3) (Lamkanfi et al., 2007). Caspase-8 can be activated by a number of apoptotic pathways, but mainly via extrinsic pathways involving FAS and immune cells (Salvesen, 2002; Stupack, 2013). In the mitochondrial (or intrinsic) pathway, released cytochrome C works with caspase-9 to activate procaspase-3 into an active caspase-3 (Li et al., 2004). Caspases-8 and -9 are down-regulated in cancers, decreasing the activation of caspase-3 (Wurstle et al., 2013; Stupack, 2013). Our results showed that the proportion of apoptotic cells was increased after CB treatment, and that caspase-3, -8, and -9 levels were increased. However, the exact mechanisms by which CB induced the expression of caspases-3, -8, and -9 must be further examined. A number of other pathways may be involved, such as the PI3K/PKB pathway (Choi et al., 2005), inhibiting glucose transporters and ion channels in some cells (Amankwah and De Boni, 1994; Wan and Xing, 1998), and decreased expression of matrix metalloproteinases-9 (Chintala et al., 1998). Furthermore, results obtained using paclitaxel, another microtubule-destabilizing agent, also showed increased levels of caspases-3 and -8 (Oyaizu et al., 1999).

In conclusion, CB blocked microfilament formation by inhibiting the polymerization of actin filaments while promoting depolymerization. It also inhibited the formation of the contractile ring and spindles and blocked cytoplasmic division, thereby inhibiting the proliferation of human glioma U251 cells and inducing U251 cell cycle arrest in the M phase. More importantly, CB induced glioma cell apoptosis, as well as increased the activities of caspases-3, -8, and -9. These results indicate the potential of CB for treating malignant gliomas.

Conflicts of interest

The authors declare no conflict of interest.

ACKNOWLEDGMENTS

Research supported by grant from the Scientific and Technological Project of Heilongjiang Province, China (#GC12C303-5).

REFERENCES

Amankwah KS and De Boni U (1994). Ultrastructural localization of filamentous actin within neuronal interphase nuclei *in situ*. *Exp. Cell Res.* 210: 315-325.

Ben-Ze'ev A (1985). The cytoskeleton in cancer cells. *Biochim. Biophys. Acta* 780: 197-212.

Buendia B, Bré MH, Griffiths G and Karsenti E (1990). Cytoskeletal control of centrioles movement during the establishment of polarity in Madin-Darby canine kidney cells. *J. Cell Biol.* 110: 1123-1135.

Chang SM, Parney IF, Huang W, Anderson FA Jr, et al. (2005). Patterns of care for adults with newly diagnosed malignant glioma. *JAMA* 293: 557-564.

Chao JI and Liu HF (2006). The blockage of survivin and securin expression increases the cytochalasin B-induced cell death and growth inhibition in human cancer cells. *Mol. Pharmacol.* 69: 154-164.

Chintala SK, Sawaya R, Aggarwal BB, Majumder S, et al. (1998). Induction of matrix metalloproteinase-9 requires a polymerized actin cytoskeleton in human malignant glioma cells. *J. Biol. Chem.* 273: 13545-13551.

Choi BH, Park JA, Kim KR, Lee GI, et al. (2005). Direct block of cloned hKv1.5 channel by cytochalasins, actin-disrupting agents. *Am. J. Physiol. Cell Physiol*. 289: C425-C436.

Cimini D, Fioravanti D, Tanzarella C and Degrassi F (1998). Simultaneous inhibition of contractile ring and central spindle formation in mammalian cells treated with cytochalasin B. *Chromosoma* 107: 479-485.

Espada A, Rivera-Sagredo, A de la Fuente JM, Hueso-Rodríguez JA, et al. (1997). New cytochalasins from the fungus *Xylaria hypoxylon*. *Tetrahedron* 53: 6485-6492.

Espindola FS, Suter DM, Partata LB, Cao T, et al. (2000). The light chain composition of chicken brain myosin-Va: calmodulin, myosin-II essential light chains, and 8-kDa dynein light chain/PIN. *Cell Motil. Cytoskeleton* 47: 269-281.

Goodenberger ML and Jenkins RB (2012). Genetics of adult glioma. *Cancer Genet*. 205: 613-621.

Haidle AM and Myers AG (2004). An enantioselective, modular, and general route to the cytochalasins: synthesis of L-696,474 and cytochalasin B. *Proc. Natl. Acad. Sci. U. S. A.* 101: 12048-12053.

Huang TS, Shu CH, Chao Y, Chen SN, et al. (2000). Activation of MAD 2 checkprotein and persistence of cyclin B1/CDC 2 activity associate with paclitaxel-induced apoptosis in human nasopharyngeal carcinoma cells. *Apoptosis* 5: 235-241.

Karp GC (2010). Cell and Molecular Biology: Concepts and Experiments. Johnm Wiley & Sons, Hoboken.

Kavallaris M (2010). Microtubules and resistance to tubulin-binding agents. *Nat. Rev. Cancer* 10: 194-204.

Kong F, Sun C, Wang Z, Han L, et al. (2011). miR-125b confers resistance of ovarian cancer cells to cisplatin by targeting pro-apoptotic Bcl-2 antagonist killer. *J. Huazhong Univ. Sci. Technolog. Med. Sci*. 31: 543-549.

Lamborn KR, Chang SM and Prados MD (2004). Prognostic factors for survival of patients with glioblastoma: recursive partitioning analysis. *Neuro.-Oncol*. 6: 227-235.

Lamkanfi M, Festjens N, Declercq W, Vanden Berghe T, et al. (2007). Caspases in cell survival, proliferation and differentiation. *Cell Death Differ.* 14: 44-55.

Laws ER, Parney IF, Huang W, Anderson F, et al. (2003). Survival following surgery and prognostic factors for recently diagnosed malignant glioma: data from the Glioma Outcomes Project. *J. Neurosurg.* 99: 467-473.

Li P, Nijhawan D and Wang X (2004). Mitochondrial activation of apoptosis. *Cell* 116: S57-S59.

Li X, Shen N, He W and Huang T (2011). The experimental research on the inhibiting impacts of RNAi on Cyclin E in breast cancer cell line. *Chinese-German J. Clin. Oncol*. 10: 502-505.

Liang YL, Wang LY, Wu H, Ma DZ, et al. (2003). PKB phosphorylation and survivin expression are cooperatively regulated by disruption of microfilament cytoskeleton. *Mol. Cell. Biochem.* 254: 257-263.

Mamelak AN and Jacoby DB (2007). Targeted delivery of antitumoral therapy to glioma and other malignancies with synthetic chlorotoxin (TM-601). *Expert Opin. Drug Deliv*. 4: 175-186.

Ohsugi M, Tokai-Nishizumi N, Shiroguchi K, Toyoshima YY, et al. (2003). Cdc2-mediated phosphorylation of Kid controls its distribution to spindle and chromosomes. *EMBO J.* 22: 2091-2103.

Oyaizu H, Adachi Y, Taketani S, Tokunaga R, et al. (1999). A crucial role of caspase 3 and caspase 8 in paclitaxel-induced apoptosis. *Mol. Cell. Biol. Res. Commun*. 2: 36-41.

Pedersen SF, Hoffmann EK and Mills JW (2001). The cytoskeleton and cell volume regulation. *Comp. Biochem. Physiol. A. Mol. Integr. Physiol.* 130: 385-399.

Pollard TD and Cooper JA (2009). Actin, a central player in cell shape and movement. *Science* 326: 1208-1212.

Salvesen GS (2002). Caspases: opening the boxes and interpreting the arrows. *Cell Death Differ.* 9: 3-5.

Skotheim JM, Di Talia S, Siggia ED and Cross FR (2008). Positive feedback of G1 cyclins ensures coherent cell cycle entry. *Nature* 454: 291-296.

Stournaras C, Stiakaki E, Koukouritaki SB, Theodoropoulos PA, et al. (1996). Altered actin polymerization dynamics in various malignant cell types: evidence for differential sensitivity to cytochalasin B. *Biochem. Pharmacol.* 52: 1339-1346.

Stupack DG (2013). Caspase-8 as a therapeutic target in cancer. *Cancer Lett.* 332: 133-140.

Wan LH and Xing M. (1998). Immunolocalization of actin in intact and DNA- and histone-depleted nuclei and chromosomes of *Allium cepa*. *Cell Res.* 8: 51-62.

Wang P, Rao J, Yang H, Zhao H, et al. (2011). PPM1D silencing by lentiviral-mediated RNA interference inhibits proliferation and invasion of human glioma cells. *J. Huazhong Univ. Sci. Technolog. Med. Sci*. 31: 94-99.

White SR, Williams P, Wojcik KR, Sun S, et al. (2001). Initiation of apoptosis by actin cytoskeletal derangement in human airway epithelial cells. *Am. J. Respir. Cell Mol. Biol.* 24: 282-294.

Wurstle ML, Laussmann MA and Rehm M (2012). The central role of initiator caspase-9 in apoptosis signal transduction and the regulation of its activation and activity on the apoptosome. *Exp. Cell Res.* 318: 1213-1220.

Yuan J, Yan R, Kramer A, Eckerdt F, et al. (2004). Cyclin B1 depletion inhibits proliferation and induces apoptosis in human tumor cells. *Oncogene* 23: 5843-5852.

Zeng X-L, Jiao M-D, Wang X-G and Hao S (1997). Actin is a constituent of the nuclear matrix and chromosome scaffold in *Physarum polycephalum*. *Acta Bot. Sin.* 9: 691-696.